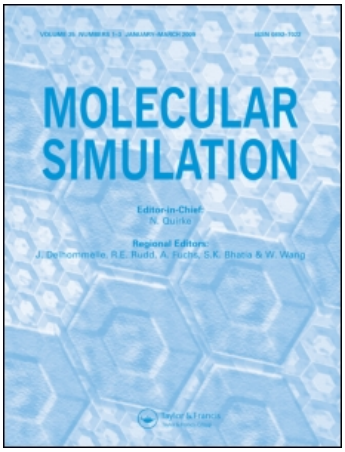

Molecular Simulation

Publication details, including instructions for authors and subscription information:
http://www.informaworld.com/smpp/title~content=t713644482

Molecular Simulations of Methane Adsorption in Silicalite

Randall Q. Snurr[a]; R. Larry June[a]; Alexis T. Bell[a]; Doros N. Theodorou[a]
[a] Department of Chemical Engineering, University of California, Berkeley, CA, USA

To cite this Article Snurr, Randall Q. , June, R. Larry , Bell, Alexis T. and Theodorou, Doros N.(1991) 'Molecular Simulations of Methane Adsorption in Silicalite', Molecular Simulation, 8: 1, 73 — 92
To link to this Article: DOI: 10.1080/08927029108022468
URL: http://dx.doi.org/10.1080/08927029108022468

Molecular Simulation, 1991, Vol. 8, pp. 73–92
Reprints available directly from the publisher
Photocopying permitted by license only

MOLECULAR SIMULATIONS OF METHANE ADSORPTION IN SILICALITE

RANDALL Q. SNURR, R. LARRY JUNE, ALEXIS T. BELL and DOROS N. THEODOROU*

Department of Chemical Engineering, University of California, Berkeley, CA 94720, USA

(*Received November 1990, accepted January 1991*)

Grand canonical ensemble Monte Carlo (GCMC) simulations of methane in the zeolite silicalite have been used to predict adsorption isotherms over a wide range of occupancies at several temperatures. The zeolite has been modeled using a detailed atomistic description, as have the methane molecules. Lennard-Jones parameters for the atomic interactions have been taken from the literature. Adsorption isotherms and heats of sorption have been predicted in good agreement with experiment. Structural features of the intracrystalline fluid have also been studied. In a complementary study, the test particle insertion method has been used to generate isotherms from molecular dynamics simulations. The results are in excellent agreement with those from GCMC.

KEY WORDS: Adsorption, chemical potential, grand canonical ensemble Monte Carlo, methane, molecular dynamics, zeolites.

INTRODUCTION

Zeolites are porous crystalline aluminosilicate materials having cavities or channels of molecular dimensions, typically 3 to 10 Å in diameter. Many of the known zeolite structures have high thermal and chemical stability, and zeolites are used extensively in catalysis, separations, and ion exchange [1] [2] [3]. In catalytic processes, the adsorption and diffusion of small sorbate molecules in the zeolite pores can significantly affect the overall catalytic performance. In separation processes it is the differences between the adsorptive and diffusive properties of the different species in a mixture which allow the separation to be achieved. Adsorption in zeolites is thus of great importance industrially. Because adsorption is controlled by molecular-level interactions, a quantitative understanding of how the adsorptive behavior of zeolite/sorbate systems is related to their molecular structure is needed in order to optimize the use of known or theoretically possible zeolite sorbents and catalysts. Computer simulations based on an atomistic description of zeolite/sorbate interactions offer great potential as a tool for zeolite design and development. When based on sound approximations, they provide a rigorous framework for the prediction of structure/property relationships in zeolites. Molecular simulation methods look particularly attractive for evaluating the properties of zeolites and other molecular sieves as the number of theoretically possible structures continues to grow [4].

*Author to whom correspondence should be addressed.

Recently we have used such molecular simulation techniques to investigate the dynamic properties and low occupancy thermodynamics of several sorbates in silicalite zeolites [5] [6]. In this paper we use the same model to study the high-occupancy thermodynamics of methane in silicalite, with prediction of adsorption isotherms being of particular interest. We compare two techniques for obtaining the isotherm: grand canonical ensemble Monte Carlo (GCMC) and the particle insertion method in conjunction with molecular dynamics (MD). From the simulations we calculate the adsorption isotherm and the heat of sorption, as well as structural features of the intracrystalline fluid. The results and computational efficiencies of the two approaches are compared, and where possible the results of both approaches are compared with experimental data.

Molecular simulations have been used in the past to study adsorption in idealized cylindrical and slit pores, as well as to study bulk fluids. There have also been several simulations of adsorption in zeolites. Stroud *et al.* conducted Monte Carlo simulations in the canonical ensemble of methane in zeolite 5A [7]. They were able to generate adsorption isotherms, isosteric heats of sorption, and heat capacities. Soto and Myers used Monte Carlo simulations in the grand canonical ensemble to study hard spheres and Lennard-Jones molecules in MS-13X [8]. Adsorption isotherms, heats of sorption, and radial distribution functions were obtained. By adjusting the potential parameters, they were able to fit the predicted isotherm for krypton in zeolite X to experimental data. Recently, Woods and Rowlinson reported grand canonical ensemble Monte Carlo simulations of xenon and methane in zeolites X and Y [9] [10]. They examined the singlet density distribution function and the distribution of occupancies in the unit cell, in addition to the adsorption isotherms and isosteric heats of adsorption. The predictions for the isotherms and isosteric heats were generally in good agreement with experimental data.

MODEL REPRESENTATION

ZSM-5, an important industrial catalyst, is available with silicon to aluminum ratios ranging from about 10 to infinity. When ZSM-5 contains virtually no aluminum, it is also known as silicalite. For the simulations performed here, the silicalite crystal is assumed to be a perfect lattice, with all framework atoms rigidly fixed in space, and to contain no defects or aluminum atoms. The crystallographic coordinates of the silicalite atoms are available from X-ray diffraction studies, and the lattice parameters are reported as 20.07 Å, 19.92 Å, and 13.42 Å for the orthorhombic phase [11]. Silicalite contains two sets of interconnected pores that are slightly elliptical in cross section and about 5.5 Å in diameter. A linear set of straight pores is directed along the [010] axis, while an intersecting set of sinusoidal pores, which follows a zig-zag path, is directed along the [100] axis. Methane is modeled as a five center Lennard-Jones molecule with bond angles and bond lengths fixed at 109.5 degrees and 1.1 Å, respectively.

The zeolite and the sorbate are assumed to interact through an effective, pairwise-additive potential between atoms of the sorbate molecules and atoms of the zeolite lattice. This interaction is largely of a London dispersion nature; long-range electrostatic interactions are assumed unimportant due to the absence of aluminum atoms in the model lattice. Trouw and Iton have performed energy minimization calcula-

tions for methane in silicalite both with and without electrostatic terms and have shown that there is only a 1% difference in the total potential energy of the methane [12]. Also, experimental isotherms for methane in ZSM-5 do not appear to be very sensitive to the aluminum content [13]. Therefore we feel justified in neglecting any small electrostatic effects. Interactions between atoms are described by a cut and shifted Lennard-Jones potential:

$$\mathscr{V}_{ij} = \begin{cases} \dfrac{A_{ij}}{r_{ij}^{12}} - \dfrac{B_{ij}}{r_{ij}^{6}} - \mathscr{V}_{ij}^{\text{shift}} & r \leqslant r_c \\ 0 & r > r_c \end{cases} \tag{1}$$

where r_{ij} is the distance between atoms i and j and

$$\mathscr{V}_{ij}^{\text{shift}} = \frac{A_{ij}}{r_c^{12}} - \frac{B_{ij}}{r_c^{6}} \tag{2}$$

The potential parameters used are given in Table 1. The methane/methane parameters are those of Murad and Gubbins [14], who adjusted the parameters to obtain good agreement between experimental data and results of their molecular dynamics simulations of liquid methane. The cutoff radius, r_c, for the methane interactions was set to 9.96 Å. This is one half the length of the shortest side of the simulation box used in the GCMC simulations and is close to the cutoff of 10.025 Å used by Murad and Gubbins. The methane/methane parameters are not the same as those used in our earlier molecular dynamics work [6]. (Our low occupancy sorption work did not involve any sorbate/sorbate interactions [5].) The parameters of Murad and Gubbins were adopted when preliminary GCMC results showed that our older parameter set did not predict the correct plateau value of the isotherm. The parameters describing the interaction of the methane carbon and hydrogen atoms with the zeolite oxygen atoms are exactly as in our earlier work [5] [6], with a cutoff radius of 13 Å and $\mathscr{V}_{ij}^{\text{shift}}$ equal to zero. It was assumed that the sorbate molecules do not interact significantly with the silicon atoms. Thus the sorbate/oxygen interaction parameters are effective parameters which take into account the interaction with the silicon atoms also. The zeolite/sorbate atom potentials were evaluated once on a fine three-dimensional grid of 0.2 Å spacing over the asymmetric unit of the unit cell and tabulated. Regions of very high potential were determined to be regions of the pore "walls" and were not included in the tabulation. During the simulations, the potential energy between a sorbate atom and the zeolite lattice was determined from the tabulated information using a three-dimensional cubic hermite polynomial interpolation algorithm [6] [15].

Table 1 Potential Parameters

Interaction Type	A_{ij} $(kJ\,mol^{-1}\,Å^{12})$	B_{ij} $(kJ\,mol^{-1}\,Å^{6})$
C–O	1134653	1535.49
H–O	147998	524.15
C–C	3401262	2406.42
H–H	70461	142.21
C–H	412242	571.18

CALCULATIONS

Calculating an adsorption isotherm for a zeolite system is a phase equilibrium problem. An adsorption isotherm shows the amount of a species taken up by the solid adsorbent phase as a function of the external gas phase pressure when the two phases are in equilibrium at a given temperature. One can predict this relationship if one knows the chemical potential in the gas phase as a function of pressure, and the chemical potential in the solid phase as a function of occupancy at the prevailing temperature. The equality of the chemical potentials and temperatures between the two phases establishes the equilibrium requirement. To obtain the isotherm from a computer simulation one can either simulate both phases or simulate the solid phase only and somehow obtain the chemical potential. Simulating two phases in direct contact is in general impractical because of the large number of molecules which would be required to avoid interfacial effects. Also, there is no need to simulate the gas phase because the thermodynamics of the gas phase is quite well understood and is adequately described by an equation of state. We have therefore chosen to simulate only the adsorbed phase. In doing such a simulation there are again two options: (1) fix the chemical potential and calculate the occupancy or (2) fix the occupancy and calculate the chemical potential. This is because the number of molecules and the chemical potential are conjugate variables. We have explored both of these possibilities with our model system. The first option corresponds to doing the simulation in the grand canonical ensemble. The second option can be accomplished by performing a molecular dynamics simulation and then calculating the chemical potential using the Widom insertion technique [16] [17]. Another method of obtaining phase equilibrium information from a computer simulation is to use the Gibbs ensemble methodology, in which both phases are simulated but not in direct physical contact [18]. The evaluation of the chemical potential is thus circumvented, but again there is no advantage in simulating the gas phase if its thermodynamics is known. Also, as pointed out by Panagiotopoulos, for adsorption in pores the Gibbs ensemble method reduces to a grand canonical ensemble simulation if the gas phase region is infinite [19].

Grand Canonical Ensemble Monte Carlo Simulations

In the grand canonical ensemble, chemical potential, volume, and temperature are fixed, while the number of molecules and the energy of the system are allowed to fluctuate. In a grand canonical ensemble Monte Carlo (GCMC) simulation, importance sampling is used to probe the statistically important regions of configuration space according to the probability density distribution for the grand canonical ensemble:

$$\rho \propto \exp\left(-kT(\mathcal{V} - \mu N) - \ln N! - 3N \ln \Lambda + N \ln V\right) \tag{3}$$

k is Boltzmann's constant, T is the temperature, $\mathcal{V}$ is the potential energy, μ is the chemical potential, N is the number of molecules in the system of volume V, and Λ is the thermal wavelength, given by

$$\Lambda = \frac{h}{(2\pi mkT)^{1/2}} \tag{4}$$

where h is Planck's constant and m is the molecular mass. To obtain a point on an adsorption isotherm from a GCMC simulation, the gas phase pressure is calculated from the fixed chemical potential using the gas phase equation of state and the number of adsorbed molecules is calculated by averaging the number of molecules in the configurations generated during the simulation. A separate simulation is required for each point on the isotherm.

We used Adams's GCMC algorithm in which configurations are generated by compound moves consisting of two parts [20] [21]. In the first part of the move, a molecule is chosen at random and given a small random displacement and a random orientation. The change in potential energy, $\Delta\mathscr{V}$, is calculated, and the move is accepted with a probability

$$p = \min\{1, \exp(-\Delta\mathscr{V}/kT)\} \tag{5}$$

by comparing with a random number between 0 and 1. In the second part of the compound move, it is decided at random to either insert an additional molecule into the system or to remove an existing molecule. The acceptance probabilities for insertions and deletions are obtained by taking the ratios of equation (3), ρ_{N+1}/ρ_N and ρ_{N-1}/ρ_N, respectively. If an insertion is to be attempted, a molecule is placed at a random location in the system, and the insertion is accepted with probability

$$p = \min\left\{1, \frac{1}{N+1}\exp(B - \Delta\mathscr{V}/kT)\right\} \tag{6}$$

where N is the number of molecules already in the system and

$$B = \frac{\mu^{ex}}{kT} + \ln\langle N\rangle \tag{7}$$

μ^{ex} is the excess chemical potential, and the total chemical potential is then

$$\mu = \mu^{ex} + \mu^{ideal} \tag{8}$$

where μ^{ideal} is the chemical potential of a gas containing the same average number of molecules per unit volume as the zeolite phase, with no interaction energy between molecules and no external field.

$$\mu^{ideal} = -kT\ln\left(\frac{V}{\langle N\rangle\Lambda^3}\right) \tag{9}$$

It should be noted that, by virtue of the phase equilibrium, B can also be written as

$$B = \frac{\mu}{kT} + \ln\frac{V}{\Lambda^3} = \int_0^P (Z-1)\frac{dP'}{P'} + \ln\left(\frac{PV}{kT}\right) \tag{10}$$

where Z is the compressibility factor of the pure gas at temperature T and pressure P', and P is the pressure of the gas phase at equilibrium. Equation (10) shows that B is known without knowing $\langle N\rangle$. Thus the inputs to the simulation are really the system volume V and temperature T and the gas phase pressure P. The chemical potential is calculated from the pressure by the equation of the state of the gas, and B is calculated from μ through Equation (10). If a deletion is to be attempted, a molecule is randomly chosen to be removed, and the removal is accepted with probability

$$p = \min \{1, N \exp(-B - \Delta\mathscr{V}/kT)\} \quad (11)$$

The maximum size of the attempted displacements was adjusted within the program to give approximately a fifty percent acceptance of the displacement moves. This maximum displacement ranged from about 0.7 Å for low occupancies at 300 K to 0.2 Å for high occupancies at 200 K. To increase the computational efficiency of the program, insertions into untabulated wall regions of the zeolite were immediately rejected. At the highest occupancies studied the insertion and deletion acceptance rates dropped to as low as 0.7 % overall, with the acceptance rates in the pores being 5.3 %. Similarly low acceptance rates were found by Woods and Rowlinson in their GCMC studies of methane in zeolites X and Y [10]. Mezei has shown that GCMC can accurately calculate average densities in liquids even with acceptance ratios for insertions and deletions as low as 0.1 % [22].

The simulation box for the GCMC simulations was taken as three unit cells stacked in the z-direction, yielding a system of 20.07 by 19.92 by 40.26 Å. The initial configuration for most runs was taken as the final configuration from the next lower point on the isotherm. Runs for the same conditions but starting from different initial occupancies always converged to the same final average occupancy, indicating an absence of any hysteresis effects. An initial configuration for the first point on each isotherm was generated by estimating the equilibrium average number of molecules, N_{est}, and randomly inserting this number of molecules into the system. The runs were allowed to equilibrate for 500,000 compound Monte Carlo moves, and averages were then taken for 1.5 to 2.5 million moves. Configurations were written to a tape file approximately after every 10 N_{est} moves, and all averaging was done in a post-processing routine using the configurations on the tape file.

Molecular Dynamics with Test Particle Insertions

In molecular dynamics (MD), trajectories in phase space are generated by integrating Newton's equations of motion for a system of molecules; this is in contrast to the Monte Carlo procedure of sampling configuration space through random moves. The microcanonical ensemble is sampled in traditional MD, so the number of molecules, the volume, and the total energy of the system are constant, while the temperature fluctuates. The details of our molecular dynamics calculations are given in an earlier paper [6]. The constraint algorithm of Edberg, Evans and Moriss [23] was used to integrate the equations of motion for all methane molecules at a given occupancy with a 1 fs time step. Configurations were written to a tape file for post-processing every 50 fs, and the length of the runs was 50 ps. The number of molecules was set at 128 or 96, and the number of unit cells was varied to yield the desired loading. The number of unit cells ranged from 8 to 32.

In the microcanonical ensemble, the excess chemical potential can be calculated from [24]

$$\mu^{ex} = -k\langle\mathscr{T}\rangle \ln[\langle\mathscr{T}\rangle^{-3/2}\langle\mathscr{T}^{3/2} \exp(-\mathscr{V}_{test}/kT)\rangle] \quad (12)$$

where $\mathscr{V}_{test}$ is the potential energy a randomly inserted test molecule would feel due to the real sorbate molecules and the zeolite. The angular brackets indicate ensemble averages, and $\mathscr{T}$ is the instantaneous kinetic temperature.

$$\mathscr{T} = \frac{\Sigma_{i=1}^{N} m v_{com,i}^2}{3Nk} \quad (13)$$

N is the number of molecules in the system, and v_{com} is the center of mass velocity. The total chemical potential is then given by equations (8) and (9) with N in place of $\langle N \rangle$. The inserted test molecules do not affect the MD simulation; they are "ghost" molecules, merely used to probe the system.

In an inhomogeneous fluid both $\mathscr{V}_{test}$ and the local density, N/V, will depend on position, but the chemical potential for a fully equilibrated system must be constant throughout the system [25]. Past simulations of inhomogeneous fluids have used generalized forms of equations (12) and (9), where $\mathscr{V}_{test}$ and N are functions of position, and then calculated the chemical potential in different regions of the system [26] [27]. For example, Heinbuch and Fischer studied a Lennard-Jones fluid in a cylindrical pore and evaluated $\mathscr{V}_{test}$ and the density of sorbate molecules in different cylindrical shells [26]. The chemical potentials in the different probe volumes were found to agree with one another except in the shell closest to the pore wall, where the high density was thought to be responsible for the inaccuracy in μ. Heinbuch and Fischer also evaluated μ over all shells together, except the shell closest to the pore, and found the result to be in agreement with the results for the smaller probe volumes. We have adopted this latter approach and evaluated μ for the entire zeolite simulation box. A regularly spaced grid of points was set up in the simulation box, and a randomly oriented fictitious molecule was inserted at each grid point into each of the configurations (every 50 fs) stored from the MD simulations [28] [29]. The grid points were at approximately 2 Å intervals in all directions. Grid points in regions where the zeolite/sorbate potential was not tabulated were considered to have infinite potential and to make no contribution to μ^{ex}. The insertions were done in a post-processing routine after the molecular dynamics runs were completed.

RESULTS

GCMC Simulations

From our GCMC simulations, adsorption isotherms for methane in silicalite at 200 and 300 K were generated. The pressures were related to the chemical potentials using the virial equation of state, and the loadings were obtained from the average number of methane molecules in the simulation box. The averages were taken over the stored configurations from the simulation. The results are compared against experimental adsorption data in Figures 1, 2, and 3 [13] [30] [31] [32]. As shown in Figure 1, our simulations predict a saturation occupancy at 200 K which is in good agreement with Yamazaki's experimental data, but tend to underpredict the amount of sorption in the pressure range of 0.05 to 0.3 atm. Sorbate/sorbate interactions are already important in this region, as evidenced by their contribution to the total internal energy. In addition to the plateau region, the very low pressure Henry's law region is captured correctly by the simulation. In Figure 4 Henry's law constants from the GCMC simulations are compared with additional experimental data and with the results of our earlier configurational integral work [33] [31] [5]. The Henry's law constant for each of the GCMC isotherms was determined by putting a line from the origin through the first point on the predicted isotherm and calculating the slope.

Figure 2 (300 K) shows characteristically the considerable disagreement that may arise in experimental measurements of zeolite isotherms. Differences in zeolite samples due to imperfections in the crystal lattice can significantly affect the volume of the micropores that is available to sorbate molecules. Our modeled zeolite is assumed to

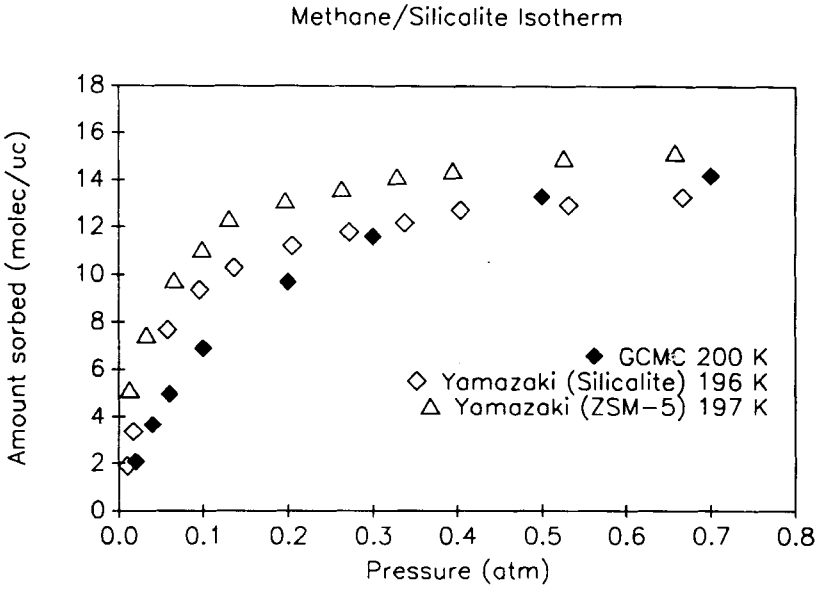

Figure 1 Adsorption isotherm of methane in silicalite at 200 K. The GCMC result is compared with experimental data of Yamazaki *et al.* (open symbols). The adsorbents used in the experimental work had Si/Al ratios of 1000 (Silicalite) and 12 (ZSM-5).

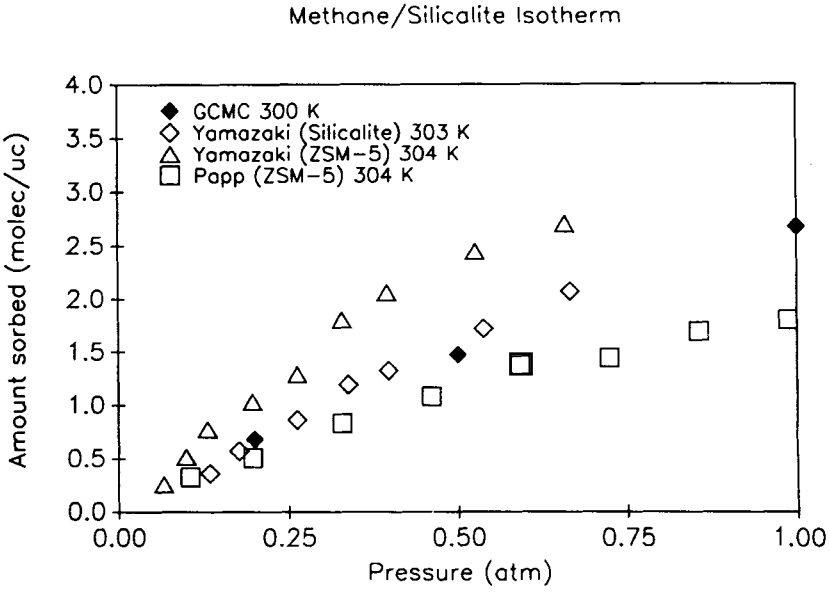

Figure 2 Low pressure adsorption isotherm of methane at 300 K. The experimental Si/Al ratios are 1000 (Silicalite) 12, (ZSM-5, Yamazaki), and 52 (ZSM-5, Papp).

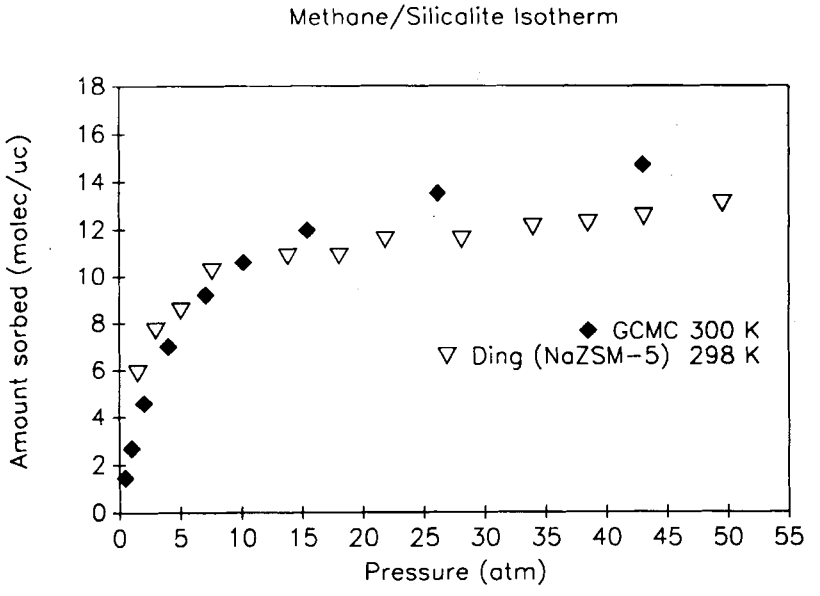

Figure 3 High pressure adsorption isotherm of methane at 300 K. The experimental data is for the sodium form of ZSM-5.

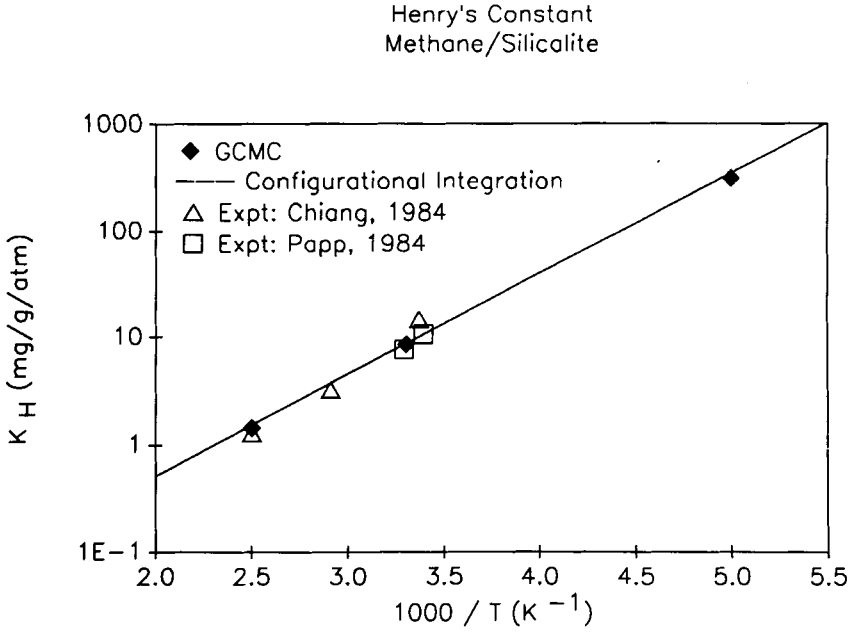

Figure 4 Comparison of Henry's Law constants from GCMC, configurational integration, and experimental data.

be a perfect crystal. The predictions are closest to Yamazaki's silicalite data. In Figure 3 simulation results are compared with the only available high pressure experimental data for sorption of methane at 300 K. It should be emphasized that the comparison is not completely legitimate, as the experimental work used the sodium form of ZSM-5. The low pressure portion of the isotherm is well captured by the simulation, while predicted occupancies in the high pressure region tend to be higher than the experimental values. This may be attributable to the sodium ions occupying part of the intracrystalline space of NaZSM-5, while this space is available for sorbate molecules in the modeled silicalite. Ding's experimental data is in the form of a Gibbs excess sorption, while the simulation gives the total sorption. We have converted Ding's data to total sorption by the prescription of Ozawa *et al.*, wherein the density of the sorbed phase is estimated empirically [34].

The statistical uncertainties in the simulation predictions for the loading of sorbate molecules were estimated by dividing each simulation run into ten blocks and calculating the standard deviation of the block averages. The uncertainties were less than 0.2 molecules per unit cell.

The average internal energy of the sorbed phase, $\langle \mathscr{U} \rangle$, is shown as a function of sorbate loading at 200 K in Figure 5. Pure unoccupied silicalite and methane in the ideal gas phase have been used as reference states in defining $\langle \mathscr{U} \rangle$. As more molecules are crowded into the zeolite, the zeolite/sorbate interaction energy per sorbate molecule rises (becomes less attractive). This is because at low occupancies the methane molecules occupy the energetically most favorable regions of the intracrystalline space, but at higher occupancies they are forced to occupy some of the less favorable regions. This effect is more than compensated by the contribution of the attractive

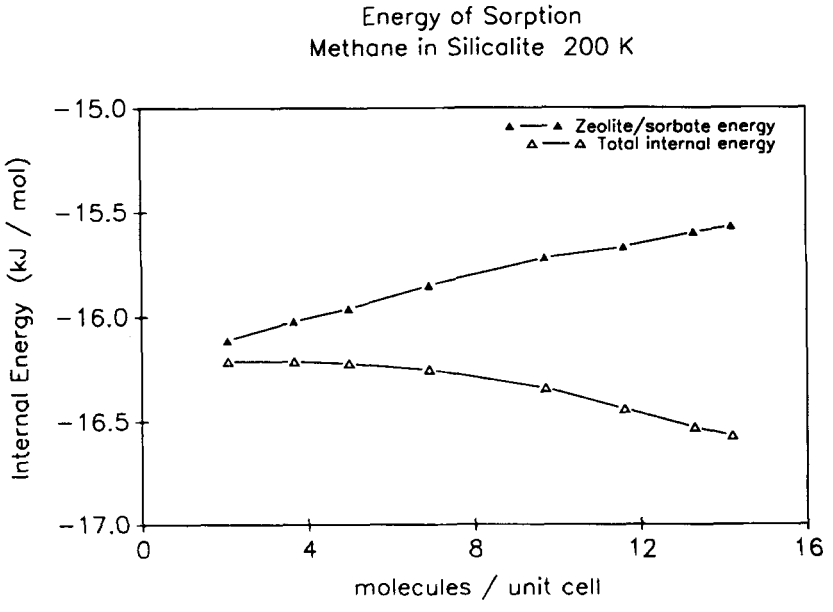

Figure 5 Internal energy of adsorbed methane molecules in silicalite at 200 K. The contribution from zeolite/sorbate interactions is shown separately.

methane/methane interaction energy, which increases with loading. The internal energy is related to the experimentally observable isosteric heat of sorption, Q_{st} as follows [6]:

$$\langle \mathscr{V} \rangle = -\frac{1}{\rho}\int_0^{\rho} Q_{st}\, d\rho' + \frac{1}{\rho}\int_0^{\rho} (H^G - H^{IG}) d\rho' + RT \tag{14}$$

In this equation, the integrations are at constant temperature along an equilibrium isotherm. The quantity ρ represents the intracrystalline occupancy, and Q_{st} is the isosteric heat at temperature T and occupancy ρ'. H^G is the molar enthalpy of the sorbate in a gas phase at equilibrium with the solid phase at temperature T and occupancy ρ', and H^{IG} is the ideal gas molar enthalpy of the sorbate at temperature T. The isosteric heat of adsorption for methane in silicalite is observed by Yamazaki to be essentially independent of occupancy at 20 kJ/mol [13]. The occupancy dependence of the simulation results noted above is within the experimental uncertainty. If Q_{st} is taken as constant and the gas phase is considered to be ideal, then equation (14) reduces to

$$\langle \mathscr{V} \rangle = -Q_{st} + RT \tag{15}$$

Using this equation we predict an isosteric heat of 18 kJ/mol, which compares favorably with the experimental result and is in full agreement with our earlier work in the Henry's law region using configurational integral techniques [5].

In addition to calculating the average loading and the average internal energy of the methane, we examined the fluctuations in the number of molecules. It can be shown

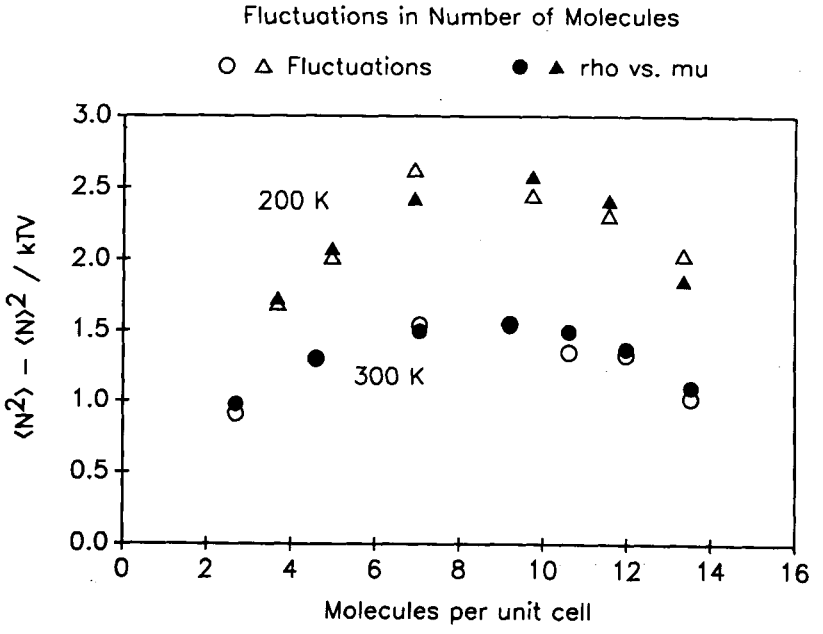

Figure 6 Fluctuations in number of molecules as a function of the average occupancy. Open symbols represent fluctuations as observed in the simulation. Filled symbols are from the derivative of ρ with respect to μ, as calculated from the predicted isotherm.

that the fluctuations are related to the slope of $\langle N \rangle$ as a function of μ [35].

$$\left(\frac{\partial \langle N \rangle}{\partial \mu}\right)_{T,V} = \frac{\langle N^2 \rangle - \langle N \rangle^2}{kT} \tag{16}$$

Both $\langle N \rangle$ and $\langle N^2 \rangle - \langle N \rangle^2$ scale with the volume of the system, so equation (16) can be rewritten as

$$\left(\frac{\partial \rho}{\partial \mu}\right)_{T,V} = \frac{\langle N^2 \rangle - \langle N \rangle^2}{kTV} \tag{17}$$

where $\rho = \langle N \rangle / V$. In Figure 6 the right hand side of the equation (17) is shown as a function of ρ for 200 and 300 K. As a check on the simulation, we also calculated the left hand side of the equation by numerically evaluating the derivative of ρ with respect to μ. The result is also shown in Figure 6. The agreement suggests that our simulations are of sufficient length to provide equilibrium information on the fluctuation properties as well as the ensemble averages of N and $\mathscr{V}$ even at high occupancies. It is seen that the fluctuations in local density are highest at intermediate loadings. The fluctuation properties can be useful in studying phase transitions such as capillary condensation. However, owing to the narrow, almost one-dimensional nature of the pores, the methane/silicalite system does not appear to exhibit any phase transition. It should be noted that both the 200 and 300 K simulations are above the critical temperature of bulk methane. The comparison in Figure 6 is a useful check on the internal consistency of the simulation. Simulations performed with 3, 6, and 12 unit cells verified that 3 unit cells was a sufficiently large simulation box; the quantities $\langle N \rangle$, $\langle \mathscr{V} \rangle$, and $(\langle N^2 \rangle - \langle N \rangle^2)/(kTV)$ all agreed to within the simulation uncertainty for the three system sizes.

Molecular Dynamics

Adsorption of methane in silicalite was also predicted from MD simulations using the particle insertion technique. In Figure 7 the results are compared with the GCMC predictions at 200 K in the form of chemical potential as a function of sorbate loading. By shifting the location of the grid of insertion points, it was shown that the chemical potential obtained from the particle insertion techique was accurate to within 0.1 kJ/mol. Using a more coarsely spaced grid yielded a wider variation in the estimates of μ for a given loading due to the poorer sampling. The point of inflection in the sigmoidal curve corresponds to the maximum in the fluctuations shown in Figure 6. The results from the two methods seem to agree well.

In addition to calculating the excess chemical potential from equation (12), one can also estimate μ^{ex} from an examination of the energy distribution functions resulting from test particle insertions. If $f(\mathscr{V})$ is the normalized distribution function of fictitious inserted molecules having potential energy $\mathscr{V}$ and $g(\mathscr{V})$ is the normalized energy distribution function of real sorbate molecules, then it can be shown that a plot of $\ln(f/g)$ versus $\mathscr{V}$ should have a slope $1/kT$ and an intercept $-\mu^{ex}/kT$ [28]:

$$\ln\left(\frac{f(\mathscr{V})}{g(\mathscr{V})}\right) = \frac{\mathscr{V}}{kT} - \frac{\mu^{ex}}{kT} \tag{18}$$

A substantial linear region in the plot is a check on the reliability of the straightforward Widom insertion calculation using Equation (12). Figure 8 shows $\ln(f/g)$ as a

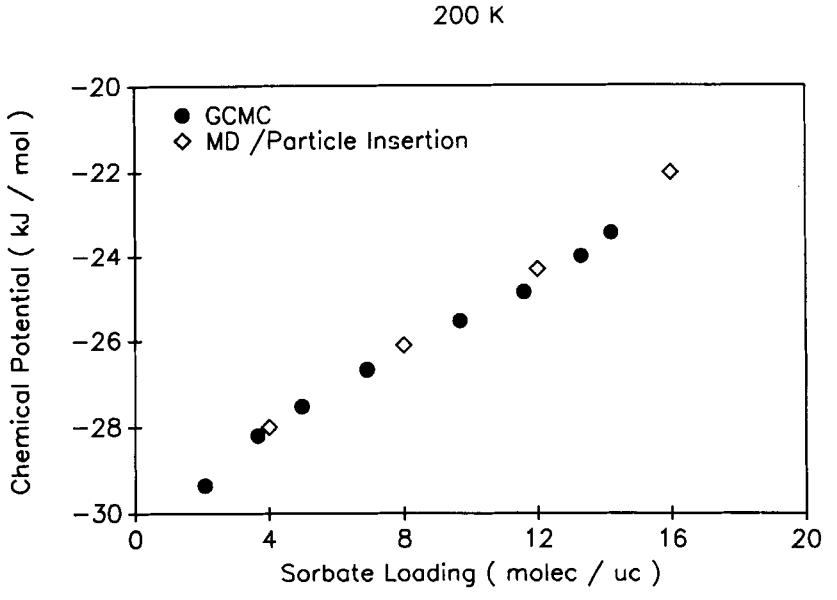

Figure 7 Chemical potential as a function of sorbate loading at 200 K. Results of the MD/Particle insertion technique are compared with the GCMC results.

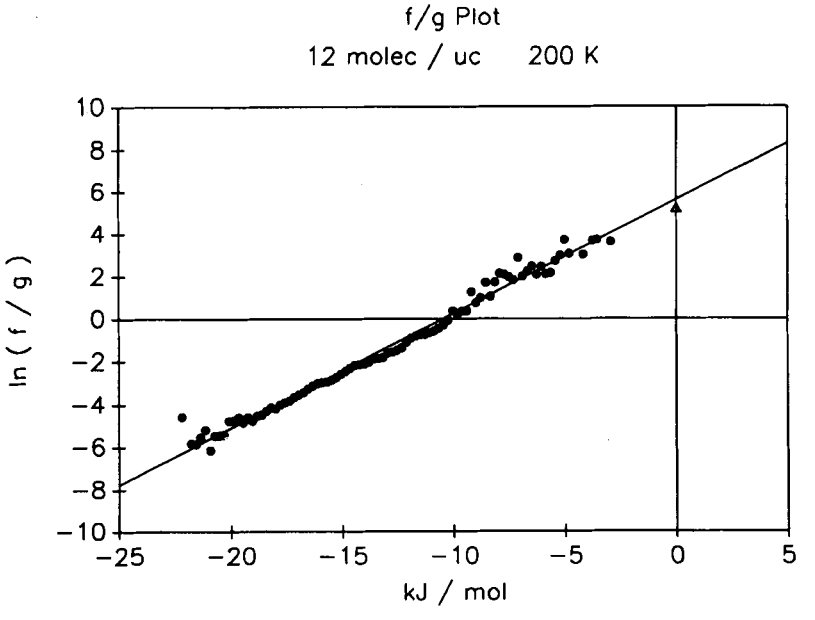

Figure 8 *f/g* plot for 12 molecules per unit cell at 200 K. The triangular point indicates the intercept expected from the results of the straightforward Widom insertions.

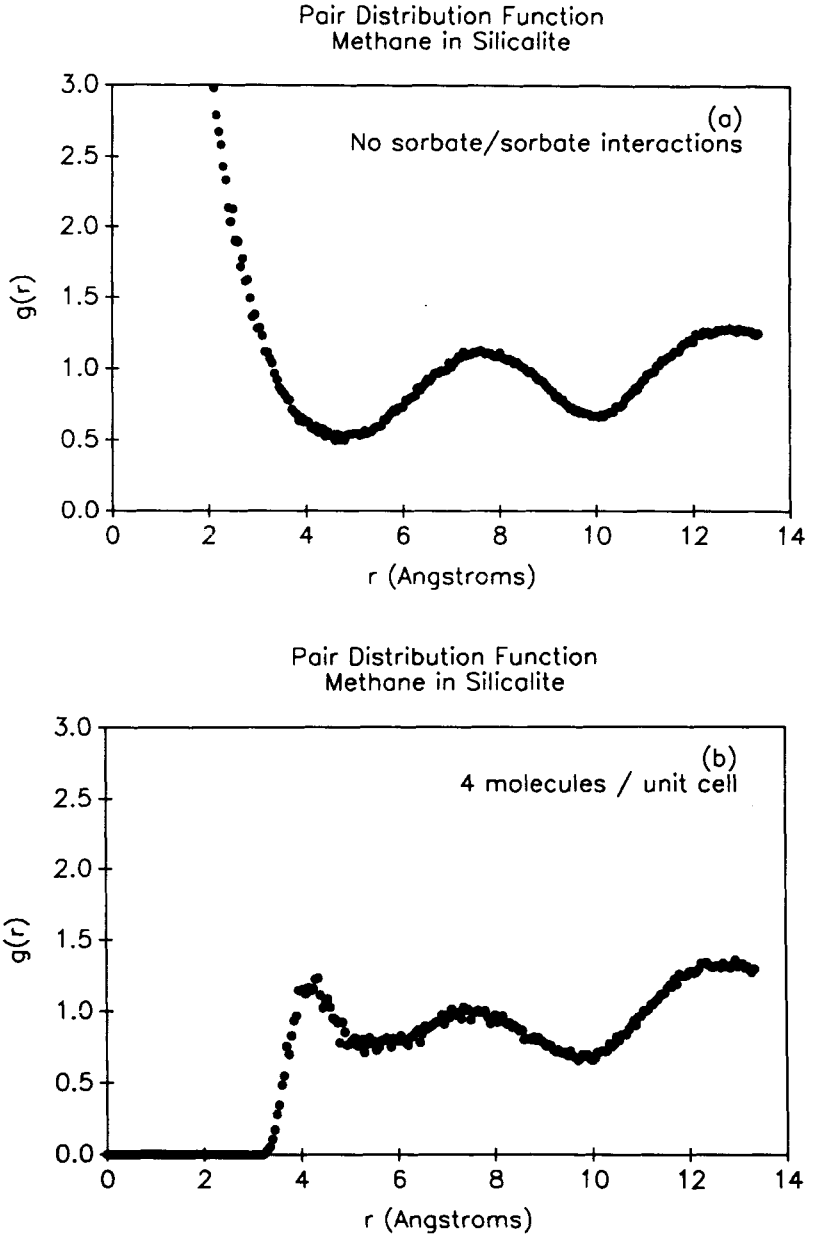

Figure 9 Pair distribution functions for methane in silicalite at 200 K. (a) no sorbate/sorbate interaction. (b) 4 molecules per unit cell.

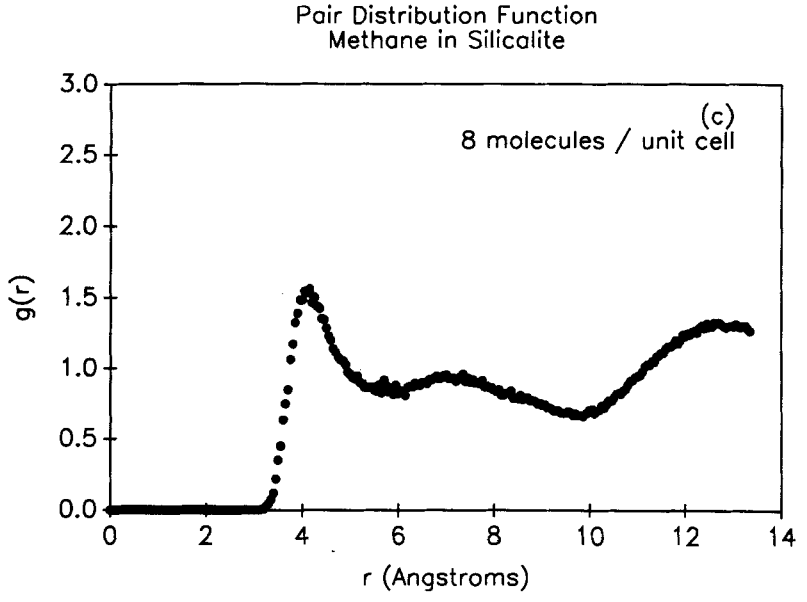

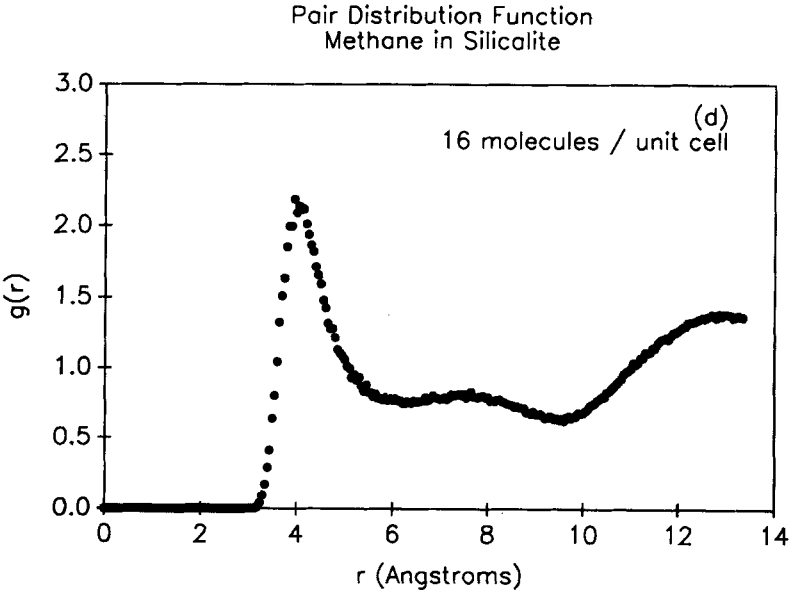

Figure 9 (*continued*) (c) 8 molecules per unit cell. (d) 16 molecules per unit cell.

function of γ for 12 molecules per unit cell at 200 K. The triangular point on the ordinate is the intercept expected from equation (12). The temperature calculated from the slope is 225 K. The linear region and the reasonable agreement of the intercept with the result from test particle insertions provide an additional check on the results shown in Figure 7. The f/g plots for 4, 8, and 16 molecules per unit cell all show similar or better agreement with the straightforward insertion calculations.

The structure of the intracrystalline fluid was studied by obtaining methane/methane pair distribution functions from the simulations. Fluid structure in a zeolite is dictated by both zeolite/sorbate and sorbate/sorbate interactions. The effects of the zeolite/sorbate interactions were isolated by performing an MD simulation in the absence of sorbate/sorbate interaction. This run was accomplished by placing 128 molecules in an 8 unit cell simulation box and then "turning off" the methane/methane potential during the simulation, so that sorbate molecules were completely decoupled and could literally pass through each other. One can obtain dynamical information at infinite dilution from such a run by tracking these "ghost" molecules, instead of following a single molecule in the zeolite crystal. In addition to improving the statistics for the infinite dilution MD run, this method allows one to calculate a pair distribution function in the absence of sorbate/sorbate interactions. The result is shown in Figure 9a. If the sorbate molecules do not interact with each other, it is expected that they will preferentially locate in the regions of the potential energy minima within the zeolite pore structure. All structure seen in Figure 9a is thus induced by the zeolite field. Because the methane molecules do not interact with one another, many methanes can occupy the same potential minimum at once. This produces a large peak in the pair distribution function at zero intermolecular separation. The other peaks are due to sorbate molecules located at *different* potential minima. The broad peak around 7.5 Å corresponds to the distance between the potential minimum in a straight channel and one in a sinusoidal channel. The peak around 13 Å has contributions from pairs of molecules both of which are in straight channels, as well as pairs where both molecules are in sinusoidal channels.

In Figures 9b through 9d, pair distribution functions for 4, 8, and 16 molecules per unit cell are shown in the presence of full sorbate/sorbate interactions. Sorbate/sorbate interactions superimpose additional structure on top of that observed in Figure 9a from the zeolite lattice alone. The most significant effect is the peak around 4 Å. This distance is close to the minimum in the methane/methane potential function (about 4.1 Å). This nearest-neighbor peak becomes more prominent as the sorbate loading is increased. The presence of dimers was also observed by Demontis *et al.* in their MD studies of methane in silicalite [36]. The spherical shell volumes probed in the pair distribution function see a highly anisotropic environment; at many angles the shell volume intersects regions of the pore walls, and no methanes will be seen. Also, because the pores are so small relative to the size of a methane molecule, a sorbate molecule located in one of the channels can see at most two neighbors. Sorbate molecules located in the channel intersections can, of course, see more than two nearest neighbors, but the channel segments rather than the intersections are more favorable for methane [6]. As a result, peaks in the orientationally averaged pair distribution function tend to be rather low. The picture that emerges from Figure 9 is that of an ordered fluid at all occupancies. The structure changes as occupancy increases, however, as the relative importance of zeolite/sorbate and sorbate/sorbate interactions changes. This picture complements and is consistent with the singlet distribution functions obtained in our previous work [5] [6].

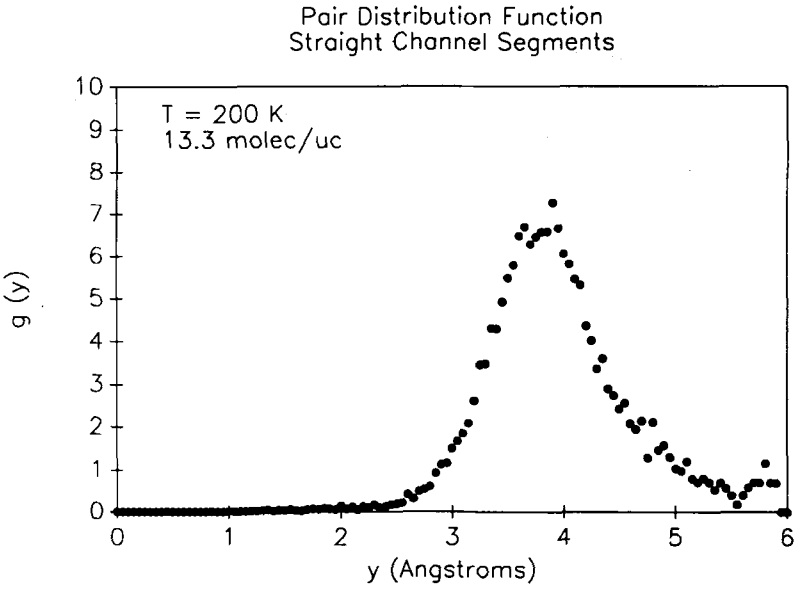

Figure 10 One-dimensional pair distribution function for methane in silicalite at 200 K and 13.3 molecules per unit cell.

One-dimensional pair distribution functions were also calculated for methane molecules lying in the straight channel segments. A typical result at high occupancy is shown in Figure 10. Sorbed molecules were first sorted as being in either the straight channels, the sinusoidal channels, or the channel intersections. One-dimensional pair distribution functions for molecules in the straight channel segments between two intersections were then determined. The separation between sorbate molecules was taken as the distance projected onto the axis of the straight channels. The anisotropy in the shell volumes for the radially averaged pair distribution functions due to the zeolite structure is not present in this one-dimensional representation. The nearest-neighbor peak is seen very clearly.

In addition to thermodynamic and structural properties, the dynamics of a system can be obtained from a molecular dynamics simulation. We have compared the diffusivities obtained from our 200 K MD simulations with the diffusivities predicted in our earlier work which used a different set of sorbate/sorbate potential parameters [6]. The predictions are fairly insensitive to the potential parameters, and both parameter sets reproduce experimental pulsed field gradient NMR measurements very satisfactorily [37].

Comparison of Computational Efficiency

Comparing the computational efficiencies of GCMC and MD for calculating an adsorption isotherm is difficult, owing to the rather different nature of the two simulation techniques. On a graph of chemical potential versus loading such as Figure 7, the error bars for GCMC are horizontal, while the error bars for MD/particle

Table 2 Comparison of Simulation Run Times

	$\langle N \rangle$ *(molecules)*	$\frac{\langle N \rangle}{V}$ *(molecules/unit cell)*	*Run Time (minutes)*
GCMC	110.6 ± 0.9	9.2 ± 0.1	77.1
MD	128	8	103.1

insertion are vertical. Thus it is difficult to say when a GCMC simulation and an MD simulation are both long enough to accomplish the same objective. In Table 2 simulation times for GCMC and MD on a Cray X-MP/14 are shown for similar numbers of molecules and loadings. The GCMC run was sufficient to calculate $\langle N \rangle / V$ to within 0.1 molecules per unit cell, while the configurations from the MD were sufficient to calculate μ to within 0.1 kJ/mol with the particle insertion method. The insertions added about 20 minutes to the time shown for the MD run. The corresponding GCMC calculation with 3 unit cells took 63 minutes to obtain the loading to within 0.2 molecules per unit cell. The grand canonical ensemble Monte Carlo was in general at least 30 % faster than the molecular dynamics, but, of course, did not provide any information on the dynamics of the system.

CONCLUSIONS

We have presented calculations for the prediction of the phase equilibrium behavior of methane in silicalite. Grand canonical ensemble Monte Carlo and molecular dynamics with test particle insertions have both been used in conjunction with the same model system. The two simulation techniques have been shown to be consistent with each other, the GCMC technique being somewhat faster computationally as a means of predicting the isotherm. However GCMC does not provide any information on the dynamics of the sorbate molecules. The particle insertion routine can be easily added to existing molecular dynamics codes, thus yielding adsorption isotherms for zeolites in addition to the usual dynamic information obtained from MD studies. The predicted adsorption isotherms and isosteric heats of adsorption are in reasonable agreement with experimental measurements. From the GCMC simulations we have seen that fluctuations in the local density are greatest at intermediate loadings of sorbate molecules. The intracrystalline fluid has been observed to be an ordered fluid at all occupancies. At low occupancies zeolite/sorbate interactions produce the main structural features, but as occupancy increases sorbate/sorbate interactions increasingly contribute to the structure of the fluid. One model with a single set of parameters has been used in this work; the model has been shown to predict correctly both dynamic and thermodynamic properties.

Acknowledgements

Support for this work was provided by W.R. Grace and Co., Conn. D.N.T. acknowledges the National Science Foundation for a Presidential Young Investigator Award,

No. DMR-8857659. The authors also thank the San Diego Supercomputer Center for a generous allocation of computer time.

References

[1] D.M. Ruthven, *Principles of Adsorption and Adsorption Processes*, Wiley Interscience, New York, 1984.

[2] R.M. Barrer, *Zeolites and Clay Minerals as Sorbents and Molecular Sieves*, Academic Press, New York, 1978.

[3] N.Y. Chen and T.F. Degnan, "Industrial catalytic applications of zeolites", *Chemical Engineering Progress*, 32 (Feb. 1988).

[4] D.E.W. Vaughan, "The synthesis and manufacture of zeolites", *Chemical Engineering Progress*, 25 (Feb. 1988).

[5] R.L. June, A.T. Bell, and D.N. Theodorou, "Prediction of low occupancy sorption of alkanes in silicalite", *J. Phys. Chem.*, **94,** 1508 (1990).

[6] R.L. June, A.T. Bell, and D.N. Theodorou, "A molecular dynamics study of methane and xenon in silicalite", *J. Phys. Chem.*, **94,** 8232 (1990).

[7] H.J.F. Stroud, E. Richards, P. Limcharoen, and N.G. Parsonage, "Thermodynamic study of the Linde sieve 5A + methane system", *J. Chem. Soc., Faraday Trans, 1*, **72,** 942 (1976).

[8] J.L. Soto and A.L. Myers, "Monte Carlo studies of adsorption in molecular sieves", *Molecular Physics*, **42,** 971 (1981).

[9] G.B. Woods, A.Z. Panagiotopoulos, and J.S. Rowlinson, "Adsorption of fluids in model zeolite cavities", *Molecular Physics*, **63,**49 (1988).

[10] G.B. Woods and J.S. Rowlinson, "Computer simulations of fluids in zeolites X and Y", *J. Chem. Soc., Faraday Trans. 2*, **85,** 765 (1989).

[11] D.H. Olson, G.T. Kokotailo, S.L. Lawton, and W.M. Meier, "Crystal structure and structure-related properties of ZSM-5", *J. Phys. Chem.*, **85,** 2238 (1981).

[12] F.R. Trouw and L.E. Iton, "Molecular dynamics simulation of the diffusion of methane in the pores of silicalite molecular sieve", in *Zeolites for the Nineties, Recent Research Reports*, J.C. Jansen, L. Moscou, and M.F.M. Post, eds, presented at the 1989 International Zeolite Conference, Amsterdam, June 1989, pp. 309–310.

[13] T. Yamazaki, I. Watanuki, S. Ozawa, and Y. Ogino, "An IR study on methane adsorbed on ZSM-5 type zeolites", *Nippon Kagaku Kaishi*, **8,** 1535 (1987).

[14] S. Murad and K.E. Gubbins, "Molecular dynamics simulation of methane using a singularity-free algorithm", *Computer Modeling of Matter, A.C.S. Symp. Ser.*, **86,** 62 (1978).

[15] M. Schultz, *Spline Analysis*, Prentice Hall, Englewood Cliffs, 1973.

[16] B. Widom, "Some topics in the theory of fluids", *J. Chem. Phys.*, **39,** 2808 (1963).

[17] B. Widom, "Potential-distribution theory and the statistical mechanics of fluids", *J. Phys. Chem.*, **86,** 869 (1982).

[18] A.Z. Panagiotopoulos, "Direct determination of phase coexistence properties of fluids by Monte Carlo simulation in a new ensemble", *Molecular Physics*, **61,** 813 (1987).

[19] A.Z. Panagiotopoulos, "Adsorption and capillary condensation of fluids in cylindrical pores by Monte Carlo simulation in the Gibbs ensemble", *Molecular Physics*, **62,** 701 (1987).

[20] D.J. Adams, "Chemical potential of hard-sphere fluids by Monte Carlo methods", *Molecular Physics*, **28,** 1241 (1974).

[21] D.J. Adams, "Grand canonical ensemble Monte Carlo for a Lennard-Jones fluid", *Molecular Physics*, **29,** 307 (1975).

[22] M. Mezei, "Grand canonical ensemble Monte Carlo study of dense liquid Lennard-Jones, soft spheres and water", *Molecular Physics*, **61,** 565 (1987).

[23] R. Edberg, D.J. Evans, and G.P. Moriss, "Constrained molecular dynamics: Simulations of liquid alkanes with a new algorithm", *J. Chem. Phys.*, **84,** 6933 (1986).

[24] M.P. Allen and D.J. Tildesley, *Computer Simulation of Liquids*, Clarendon Press, Oxford, 1987.

[25] B. Widom, "Structure of interfaces from uniformity of the chemical potential", *Journal of Statistical Physics*, **19,** 563, (1978).

[26] U. Heinbuch and J. Fischer, "On the application of Widom's test particle method to homogeneous and inhomogeneous fluids", *Molecular Simulation*, **1,** 109 (1987).

[27] A. Cheng and W.A. Steele, "Computer simulation study of the chemical potential of argon adsorbed graphite", *Molecular Simulation*, **4,** 349 (1990).

[28] J.G. Powles, W.A.B. Evans, and N. Quirke, "Non-destructive molecular-dynamics simulation of the chemical potential of a fluid", *Molecular Physics*, **46,** 1347 (1982).
[29] D. Fincham, N. Quirke, and D.J. Tildesley, "Computer simulation of molecular liquid mixtures. I. A diatomic Lennard-Jones model mixture for CO_2/C_2H_6" *J. Chem. Phys.*, **84,** 4535 (1986).
[30] T. Yamazaki, I. Watanuki, S. Ozawa, and Y. Ogino, "Infrared spectra of methane adsorbed by ion-exchanged ZSM-5 zeolites", *Langmuir*, **4,** 433 (1988).
[31] H. Papp, W. Hinsen, N.T. Do, and M. Baerns, "The adsorption of methane on H-ZSM-5 zeolite", *Thermochimica Acta*, **82,** 137 (1984).
[32] T. Ding, S. Ozawa, and Y. Ogino, "Adsorption equilibria of methane, nitrogen, and carbon dioxide on ZSM-5", *Zhejiang Daxue Xuebao*, **22,** 124 (1988).
[33] A.S. Chiang, A.G. Dixon, and Y.H. Ma, "The determination of zeolite crystal diffusivity by gas chromatography - II. Experimental", *Chemical Engineering Science*, **39,** 1461 (1984).
[34] S. Ozawa, S. Kusumi, and Y. Ogino, "Physical adsorption of gases at high pressure IV. An improvement of the Dubinin-Astakhov adsorption equation", *Journal of Colloid and Interface Science*, **56,** 83 (1976).
[35] T.L. Hill, *An Introduction to Statistical Thermodynamics*, Dover, New York, 1986.
[36] P. Demontis, E.S. Fois, G.B. Suffritti, and S. Quartieri, "Molecular dynamics studies on zeolites. 4. Diffusion of methane in silicalite", *J. Phys. Chem.*, **94,** 4329 (1990).
[37] H. Jobic, M. Bee, J. Caro, M. Bülow, J. Kärger, "Molecular self-diffusion of methane in zeolite ZSM-5 by quasi-elastic neutron scattering and nuclear magnetic resonance pulsed field gradient technique", *J. Chem. Soc., Faraday Trans 1*, **85,** 4201 (1989).